Journal of Alloys and Compounds 646 (2015) 73–79

Contents lists available at ScienceDirect

Journal of Alloys and Compounds

journal homepage: http://www.elsevier.com/locate/jalcom

Preparation and characterization of the non-stoichiometric La–Mn perovskites

Zhiming Gao [a, *], Huishu Wang [a], Hongwei Ma [a], Zhanping Li [b]

[a] School of Chemistry, Beijing Institute of Technology, Liangxiang East Road, Beijing 102488, China
[b] Analysis Center, Tsinghua University, Beijing 100084, China

ARTICLE INFO

Article history:
Received 25 March 2015
Received in revised form
26 May 2015
Accepted 5 June 2015
Available online 12 June 2015

Keywords:
Non-stoichiometric perovskite
XRD
XPS
Lattice vacancy
Methane

ABSTRACT

Six La–Mn oxide samples with La/Mn atomic ratio x = 1.03–0.56 (denoted as sample LaxMn) were prepared by the citrate method with calcination at 700 °C for 5 h, and characterized by X-ray diffraction (XRD), N_2 adsorption–desorption, temperature programmed reduction (TPR) and X-ray photoelectron spectroscopy (XPS). It is confirmed that the four samples with La/Mn atomic ratio at 1.03–0.72 are all single phase perovskites by XRD patterns. Lattice parameters of the perovskites are varying with the La/Mn atomic ratio. As the La/Mn atomic ratio further lowers to 0.63 and 0.56, Mn_3O_4 phase is formed besides the main phase of perovskite. Lattice vacancy at the A-sites of the perovskites is present for all the six samples, and there are an appreciable number of Mn^{4+} ions in the perovskite crystal according to the refinement results of the Rietveld method. XPS analyses indicate that Mn ions are enriched on the surfaces of all the samples. In addition, catalytic activity for methane oxidation is in an order of sample $La_{0.89}Mn > La_{1.03}Mn > La_{0.81}Mn > La_{0.72}Mn > La_{0.63}Mn > La_{0.56}Mn$.

1. Introduction

Perovskite-type oxide has a general formula ABO_3, where usually La^{3+} ions occupy at the lattice A-sites and ions of a transition metal (Mn, Fe, Co etc.) occupy at the lattice B-sites [1]. When La^{3+} ions were substituted partially by other metallic ions at a lower valence state such as Ca^{2+} and Sr^{2+} ions, lattice oxygen vacancy would be formed together with a part of transition metal ions changing into a higher valence state in the crystal structure to maintain electrical neutrality [1–5]. Oxygen in gas phase can adsorb at the surface lattice oxygen vacancy, forming adsorbed oxygen species either neutral or charged [1,3,6]. Perovskite-type oxides are thus effective for catalytic combustion of hydrocarbons and purification of exhaust gas of vehicles [1–8]. Arai et al. estimated the respective contribution of surface adsorbed oxygen species and surface lattice oxygen as catalytically active species for methane oxidation at reaction temperatures 450 °C–650 °C, and argued that the contribution of surface lattice oxygen increased with reaction temperature increasing [8]. When charged oxygen species, including surface lattice oxygen and charged surface adsorbed oxygen, are catalytically active species, its consumption and regeneration is accompanied by cycling of valence state of neighboring transition metal ions such as $B^{3+} \leftrightarrow B^{4+}$ and/or $B^{2+} \leftrightarrow B^{3+}$ [1,3,6]. The ease at the cycling of valence state is dependent on kind of transition metal. Hence, kind of transition metal ions at the B-sites influences catalytic activity of perovskite-type oxides greatly [6,8].

There are many papers regarding preparation and property of the stoichiometric perovskites with molar number of the A ions equal to that of the B ions, including the case where La^{3+} ions are partially substituted by Ca^{2+} or Sr^{2+} ions etc [1–5,8–10]. Only a few of papers are published on preparation and characterization of the non-stoichiometric perovskites with La/B (B = Fe, Mn) atomic ratio unequal to unity to our knowledge [6,11–15]. Faye et al. reported that their La–Fe oxide samples with La/Fe atomic ratio at 0.94 and 0.83 (the La/Fe atomic ratios are measured by ICP) are both single phase perovskites according to XRD patterns [6]. And it is claimed that the low La/Fe atomic ratios did not result in formation of cationic vacancies in the perovskite structure [6]. Delmastro et al. synthesized $La_{(1-n)}FeO_{(3-1.5n)}$ perovskites with n = 0.0, 0.1, 0.2 and 0.3 (nominal value of the fed chemicals) at calcination temperature of 600 °C and confirmed that all the samples are monophasic by XRD patterns [11]. But, for the sample with n = 0.3, Moessbauer spectroscopy detected presence of ironic oxide besides the

* Corresponding author.
E-mail address: zgao@bit.edu.cn (Z. Gao).

http://dx.doi.org/10.1016/j.jallcom.2015.06.044
0925-8388/

perovskite phase [11]. They proposed that the excess ironic oxide in the $n > 0$ samples corresponds to presence of Fe–O polyhedra at the crystallite surface, and in such a way the decrease of La/Fe atomic ratio does not affect the interior of the structure with a regular perovskite lattice [11]. They further confirmed by increasing calcination temperature from 600 °C to 1200 °C that XRD peaks of Fe_2O_3 phase appear at 800 °C first and then increase their intensity at higher temperatures [11].

It is confirmed that perovskite $LaMnO_{3.158}$ is not an anion-excess perovskite and just a conventional written form; it has an actual composition $La_{0.95}Mn_{0.95}O_3$ with randomly distributed La and Mn vacancies at the cationic lattice sites and a filled sublattice of anions in the crystal structure [13]. It is reported that the sample with La/Mn atomic ratio of 0.95 (the La/Mn atomic ratio was measured by ICP) and calcined at 800 °C is single phase perovskite [14]. Its real composition can be written as $La_{0.95}Mn^{3+}_{0.73}Mn^{4+}_{0.27}O_{3.06}$ in a conventional way, and exactly is in the form of $La_{0.931}Mn^{3+}_{0.716}Mn^{4+}_{0.265}O_3$ with lattice vacancies at the A-sites and the B-sites and a filled sublattice of lattice oxygen anions (O^{2-}) [14]. Besides, the sample with La/Mn atomic ratio of 0.91 (measured by ICP) and calcined at 800 °C is also reported to be single phase perovskite [15]. In the present work, a series of La–Mn oxide samples with feed La/Mn atomic ratio at 1.03–0.56 (measured by XRF) were prepared. Phase composition of the samples was estimated by the Rietveld refinement method. Surface composition was analyzed by XPS. Catalytic activity for methane oxidation of the samples was also evaluated.

2. Experimental

2.1. Preparation of La–Mn oxides

Citrate method was adopted to prepare La–Mn oxides from metal nitrates (Guoyao Chemicals, China). At first, an aqueous solution of lanthanum nitrate and manganese nitrate was added dropwise into an aqueous citric acid solution (the molar ratio of the citric acid to the total metallic ions was fixed at 0.5) under rigorous stirring, and stirring was kept for 30 min after the addition completed. Then, the citrate solution was heated in a rotary evaporator at 80 °C and vacuum degree of 0.08 MPa for 25 min, where a viscous liquid was obtained. The viscous liquid was dried in an oven at 80 °C for 5 h and subsequently at 110 °C for 2 h. At last, the dried sample was calcined in a muffle furnace at 700 °C for 5 h. In this way six samples were prepared with feed La/Mn atomic ratio at 1.03, 0.89, 0.81, 0.72, 0.63 and 0.56 (measured by X-ray fluorescence spectroscopy, XRF-1800, Shimadzu), respectively. These samples are thus denoted as La*x*Mn, in which the variable *x* is the La/Mn atomic ratio of the samples.

2.2. Characterizations

Phase identification of the samples was performed on an X-ray diffractometer (D8 Advance, Bruker) with Cu K*a* irradiation at 40 kV and 40 mA. The Rietveld refinement method implemented in the TOPAS software package was used to estimate phase composition of the samples and crystallite size of the perovskite phase.

Specific surface area (SSA) of the samples was measured on a SSA instrument (JW-DA, Beijing JWGB, China). At first the samples were degassed at 150 °C for 1 h in high vacuum, and then allowed to adsorb N_2 at liquid nitrogen temperature (−196 °C) under a relative pressure of $p/p_0 = 0.06–0.30$. The BET equation was used to calculate SSA value.

Reducibility of the samples was measured by temperature programmed reduction (TPR) method on a TPR instrument (PX200, Tianjin Pengxiang, China) equipped with a thermal conductivity detector (TCD), where a reducing gas of 10%H_2/Ar was set at 40 ml/min, temperature was ramped to 900 °C at 10 °C/min, and sample powder was fixed at 50.0 mg at each run.

Surface elemental composition of the samples was analyzed on an X-ray photoelectron spectrometer (PHI Quantera) with monochromatized Al Kα radiation. The base pressure of the instrument was 2×10^{-9} Torr. Curve-fitting for the XPS peaks, which were calibrated with the binding energy of adventitious carbon C1s = 284.8 eV, was performed with a Gaussian–Lorentzian profile.

2.3. Catalytic activity for methane oxidation

Catalytic activity for methane oxidation of the La–Mn oxide samples as catalysts (200 mg, 40–60 mesh) was evaluated in a continuous flow fixed-bed quartz tube reactor (8 mm i.d.) at atmospheric pressure. Total flow rate of the feed gas was 200 ml/min, in which methane was 2.0 vol%, oxygen gas 16.8 vol%, nitrogen as balance gas. The catalytic reaction was carried out at 500 °C–600 °C in temperature rising way. After 1 h stabilization of the reaction at each the reaction temperatures, reaction products were analyzed on a gas chromatograph (Shanghai Kechuang, China). Then reaction temperature was elevated to the next higher value. CO_2 was the sole carbon-containing product.

3. Results and discussion

3.1. Phase composition and crystallite size

Fig. 1 shows XRD patterns of the six La–Mn oxide samples. All samples display clearly characteristic peaks of perovskite phase. Among the six samples, the four samples with La/Mn atomic ratio at 1.03, 0.89, 0.81 and 0.72 (measured by XRF) are single phase perovskites. The other two samples with La/Mn atomic ratio at 0.63 and 0.56 (measured by XRF) are composed of perovskite as the main phase and Mn_3O_4 as the minor phase. XRD patterns in Fig. 1 are fitted by the Rietveld refinement method, and the results are listed in Tables 1 and 2. In the refinement, occupancy of lattice oxygen anion is fixed at one [13], and occupancies of two of the three types of cation (La^{3+}, Mn^{3+}, Mn^{4+}) are refined with the confinement of electrical neutrality in the perovskite crystal. Mass balance on the La/Mn atomic ratios is not considered in the refinement, since highly dispersed MnO*x* and/or La_2O_3 species may

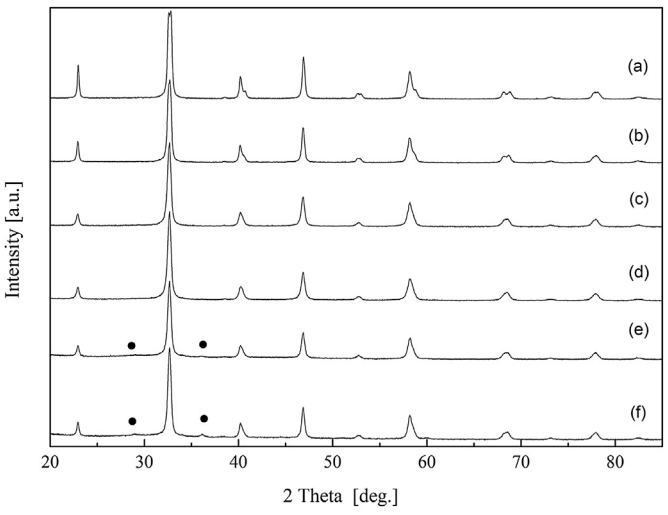

Fig. 1. XRD patterns of the samples with feed La/Mn atomic ratio at 1.03 (a), 0.89 (b), 0.81 (c), 0.72 (d), 0.63 (e) and 0.56 (f). The black circle denotes Mn_3O_4 phase.

Table 1
Phase composition of the samples and crystallite size of the perovskite phase estimated by the Rietveld method, specific surface area of the samples.

Sample	Phase composition (wt%)		Crystallite size of perovskite phase (nm)	Specific surface area (m^2/g)
$La_{1.03}Mn$	Perovskite	100	47.6 ± 0.5	6.1
$La_{0.89}Mn$	Perovskite	100	46.2 ± 0.5	7.0
$La_{0.81}Mn$	Perovskite	100	33.5 ± 0.4	13.5
$La_{0.72}Mn$	Perovskite	100	31.5 ± 0.3	17.4
$La_{0.63}Mn$	Perovskite	96.4 ± 0.3	33.8 ± 0.3	13.1
	Mn_3O_4	3.6 ± 0.3		
$La_{0.56}Mn$	Perovskite	89.5 ± 0.3	37.4 ± 0.4	13.0
	Mn_3O_4	10.5 ± 0.3		

not be detectable by XRD [16]. It is found that the La/Mn atomic ratio derived from the phase composition in Tables 1 and 2 is actually higher slightly than that measured by XRF for all the six samples, suggesting presence of MnO*x* species that is not detectable by XRD. This is similar to that observed for the La–Fe oxide samples [6,11] and for the La–Mn oxide samples [14,15]. Faye et al. reported that the La–Fe oxide sample with La/Fe atomic ratio at 0.83 (measured by ICP) is single phase perovskites according to XRD pattern [6]. Delmastro et al. confirmed a La–Fe oxide sample with La/Fe atomic ratio at 0.7 (nominal value of the fed chemicals) being single phase perovskite based on XRD pattern, although Moessbauer spectroscopy detected presence of ironic oxide [11]. They thus proposed that the excess ironic oxide in the sample corresponds to presence of Fe–O polyhedra at the crystallite surface [11]. For La–Mn oxide sample, single phase perovskite was confirmed at La/Mn atomic ratio of 0.91 (measured by ICP) [15]. In the present work, it is confirmed by XRD patterns that the samples with La/Mn atomic ratio at 1.03–0.72 are all single phase perovskites. And as the La/Mn atomic ratio was further lowered to 0.63, formation of Mn_3O_4 phase was observed. But, although Mn_3O_4 phase is formed at the La/Mn atomic ratios of 0.63 and 0.56, there are still MnO*x* species present in the samples that is not detectable by XRD as mentioned above.

As well known, manganese element is stable at valence state of +4. So, an appreciable number of Mn^{4+} ions can be present in La–Mn perovskite crystal, with molar ratio of $Mn^{4+}/(Mn^{3+} + Mn^{4+})$ equal to 0.27 [14] or 0.34 [17]. In Table 2, for the four samples with La/Mn atomic ratio at 1.03, 0.89, 0.81 and 0.72, it is seen that the molar ratio of $Mn^{4+}/(Mn^{3+} + Mn^{4+})$ in the perovskite crystals is varying within 0.25–0.40. While, for the other two samples with La/Mn atomic ratio at 0.63 and 0.56, molar ratio of $Mn^{4+}/(Mn^{3+} + Mn^{4+})$ in the perovskite crystals is relatively low, at ca. 0.12, which is in contrast with presence of Mn_3O_4 phase in the two samples. Besides, for the samples $La_{1.03}Mn$ and $La_{0.89}Mn$, lattice vacancy at the B-sites may be present due to the value of ϕ_B (lattice vacancy at the B-sites) equal to or slightly higher than the error in occupancy of Mn ions. Presence of lattice vacancy at the A-sites should be certain, because the value of ϕ_A (lattice vacancy at the A-sites) is much higher than the error in occupancy of La^{3+} ions. Among the six samples, the sample $La_{1.03}Mn$ has the smallest value of ϕ_A, corresponding to the highest occupancy of La^{3+} ions at 0.982. The other five samples have a relatively large value of ϕ_A within 0.06–0.10 due to the large La-deficiency in the fed chemicals. Varying of lattice parameters of the perovskite crystals is also worth noting in Table 2. It is seen that as La/Mn atomic ratio lowers from 1.03 to 0.72, the parameter (*a*) decreases slightly and meanwhile the parameter (*c*) increases significantly. When La/Mn atomic ratio is further lowered to 0.63 and 0.56, the parameter (*a*) recovers to a high value and the parameter (*c*) maintains at a high value. These results indicate that the La/Mn atomic ratio in the fed chemicals affects crystal formation and growth of products of the solid reactions in the sample preparation.

Specific surface area (SSA) of the six La–Mn oxide samples is listed in Table 1. It is seen that the SSA value increases with the La/Mn atomic ratio decreasing from 1.03 to 0.72. At the La/Mn atomic ratios of 0.63 and 0.56, SSA value is constant at about 13 m^2/g. Crystallite size of the perovskite phase (estimated by the Rietveld method) varies with the La/Mn atomic ratio. The varying is consistent with the SSA value. That is, smaller size of the perovskite crystallites results in a larger SSA value for the samples. In addition, thickness at the (211) plane (2theta = 36.1°) of Mn_3O_4 crystallites was estimated by the Scherrer equation for the samples $La_{0.63}Mn$ and $La_{0.56}Mn$. It is found that the thickness is ca. 17.5 nm for the two samples.

Fig. 2 shows TPR profiles of the six La–Mn oxide samples. Similarly to the reports [16–18], the low temperature reduction peaks within ca. 300 °C–500 °C correspond to reduction of Mn^{4+} ions into Mn^{3+} ions and reduction of a part of Mn^{3+} ions into Mn^{2+} ions, the high temperature reduction peaks above 650 °C correspond to reduction of Mn^{3+} ions into Mn^{2+} ions. The final state of the TPR processes is mixture of MnO and La_2O_3 [16–18]. For the samples $La_{0.63}Mn$ and $La_{0.56}Mn$, a higher peak appears at around 400 °C, which corresponds to reduction of Mn_3O_4 phase [19]. It is also seen that the sample $La_{1.03}Mn$ has a relatively lower reducibility, especially in the high temperature reduction step, in comparison with the other five samples. This would be due to the low value of ϕ_A at the A-sites of the sample. It is reported that the high temperature reduction peak shifts to a lower temperature as the *x*

Table 2
Occupancy of cation in perovskite structure and lattice parameter of perovskite phase estimated by the Rietveld method.

Sample	Occupancy of cation[a]					Lattice parameter (Å)[b]	
	La^{3+}	ϕ_A	Mn^{3+}	Mn^{4+}	ϕ_B	*a*	*c*
$La_{1.03}Mn$	0.982 ± 0.008	0.018	0.61 ± 0.06	0.30 ± 0.04	0.08	5.4975 ± 0.0003	13.3053 ± 0.0007
$La_{0.89}Mn$	0.927 ± 0.007	0.073	0.57 ± 0.05	0.38 ± 0.04	0.05	5.4962 ± 0.0002	13.3279 ± 0.0007
$La_{0.81}Mn$	0.924 ± 0.008	0.076	0.74 ± 0.06	0.25 ± 0.04	~0	5.4918 ± 0.0004	13.3488 ± 0.0011
$La_{0.72}Mn$	0.898 ± 0.007	0.102	0.64 ± 0.05	0.35 ± 0.04	~0	5.4895 ± 0.0004	13.3536 ± 0.0011
$La_{0.63}Mn$	0.934 ± 0.008	0.066	0.91 ± 0.06	0.12 ± 0.04	~0	5.4946 ± 0.0003	13.3571 ± 0.0010
$La_{0.56}Mn$	0.938 ± 0.007	0.062	0.89 ± 0.06	0.13 ± 0.04	~0	5.4953 ± 0.0003	13.3564 ± 0.0009

[a] ϕ_A and ϕ_B are lattice vacancy at the A-sites and the B-sites of the perovskites, respectively.
[b] On rhombohedral symmetry.

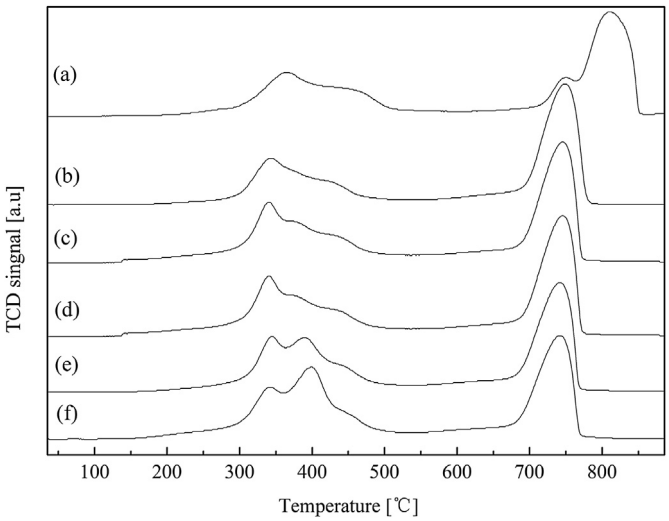

Fig. 2. TPR curves of the samples with feed La/Mn atomic ratio at 1.03 (a), 0.89 (b), 0.81 (c), 0.72 (d), 0.63 (e) and 0.56 (f).

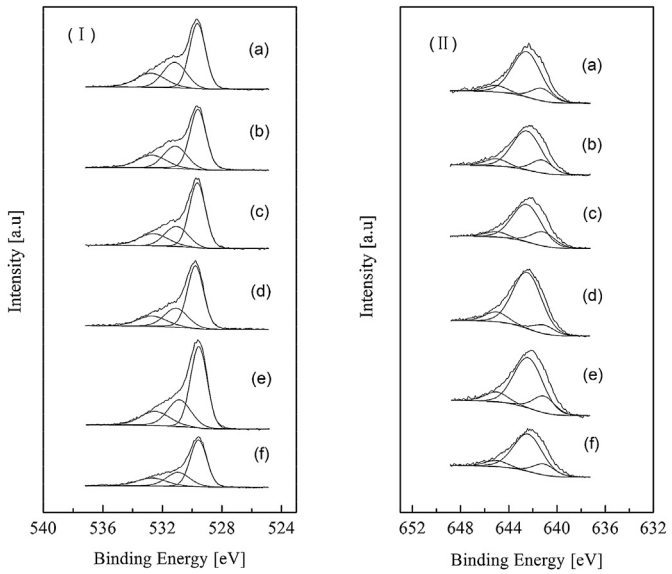

Fig. 3. XPS spectra of O1s (I) and Mn2$p_{3/2}$ (II) of the samples with feed La/Mn atomic ratio at 1.03 (a), 0.89 (b), 0.81 (c), 0.72 (d), 0.63 (e) and 0.56 (f).

value increases for the samples $La_{1-x}Sr_xMnO_3$ ($0.0 \leq x \leq 0.5$) [16], suggesting presence of more defects at the lattice A-sites can induce an easier reduction for the samples.

3.2. Elemental composition at the surface

XPS spectra were recorded for the six La–Mn oxide samples. Surface composition (excluding carbon element) and surface La/Mn atomic ratio are listed in Table 3 together with the binding energies of the core electrons of O1s and Mn2$p_{3/2}$. It is clear that the surface La/Mn atomic ratio is lower than that of the whole bulk measured by XRF for all the samples, indicating that Mn ions are enriched on the surfaces of the samples. This is in agreement with the literatures [16,20]. Ponce et al. reported a surface La/Mn atomic ratio of ca. 0.78 for the sample with the feed La/Mn atomic ratio at 1.01 [16]. Machocki et al. reported a surface La/Mn atomic ratio of 0.28 for the sample with the feed La/Mn atomic ratio at 1.07 [20]. XPS spectra of O1s and Mn2$p_{3/2}$ of the samples are shown in Fig. 3. In Fig. 3 (I), the peak at 529.6 eV is generated from surface lattice oxygen anions (O^{2-}), and the peak at ca. 531.1 eV can be assigned to surface adsorbed oxygen species (such as O_2^{2-} and O^-), surface hydroxyls and surface carbonate ions [15,16,21,22], the peak at ca. 532.6 eV can be assigned to the weakly adsorbed species [16,21]. In Fig. 3 (II), three component peaks are resolved for the spectra of Mn2$p_{3/2}$ [15,16,20]. The component peak at ca. 641.2 eV corresponds to Mn^{3+} ions and/or Mn ions in Mn_3O_4, the one at ca. 642.5 eV corresponds to Mn^{4+} ions, and the last one at 645.0 eV is a satellite peak. The deconvolution for the peaks has ambiguity in the recognition of Mn ions at the different valence states due to the small differences in their binding energies [16,23]. Nevertheless, it is certain that surface Mn^{4+} ions are present in an appreciable quantity. This is because Mn^{4+} ions are already present in the perovskite crystal [14,17]. And also it is understood that surface Mn^{3+} ions can be converted into Mn^{4+} ions when there are adsorbed oxygen species at the surface getting electrons from the neighboring Mn^{3+} ions [3,6].

Table 3
Surface composition and surface La/Mn atomic ratio estimated by XPS and binding energies (eV) of the core electrons of the samples.[a]

Sample	Surface composition (at%)			Surface La/Mn	Binding energy of O1s	Binding energy of Mn2$p_{3/2}$
	O	La	Mn			
$La_{1.03}Mn$	72.5	12.9	14.5	0.89	529.6 (51.2) 531.2 (28.0) 532.8 (20.8)	641.3 (15.8) 642.5 (75.4) 645.0 (8.8)
$La_{0.89}Mn$	74.2	11.3	14.5	0.78	529.6 (53.3) 531.1 (26.3) 532.7 (20.4)	641.2 (18.3) 642.5 (70.7) 645.0 (11.0)
$La_{0.81}Mn$	76.4	9.3	14.3	0.65	529.6 (56.3) 531.1 (24.0) 532.6 (19.7)	641.2 (22.2) 642.5 (69.4) 645.0 (8.4)
$La_{0.72}Mn$	76.8	7.9	15.2	0.52	529.6 (54.9) 530.9 (27.2) 532.5 (17.9)	641.1 (18.7) 642.4 (69.7) 645.0 (11.6)
$La_{0.63}Mn$	71.4	9.1	19.4	0.47	529.8 (57.4) 531.1 (25.5) 532.7 (17.2)	641.1 (9.5) 642.5 (78.8) 645.0 (11.7)
$La_{0.56}Mn$	74.5	6.8	18.8	0.36	529.6 (56.6) 531.0 (25.4) 532.7 (18.0)	641.1 (16.6) 642.4 (73.7) 645.0 (9.8)

[a] Peak percentages of the components are in parenthesis.

3.3. Catalytic activity for methane oxidation

Catalytic activities for methane oxidation of the six La–Mn oxide samples as catalysts are compared in Fig. 4 at reaction temperatures 500 °C–600 °C. It is seen that methane conversion is in the order of sample $La_{0.89}Mn > La_{1.03}Mn > La_{0.81}Mn > La_{0.72}Mn > La_{0.63}Mn > La_{0.56}Mn$. This order is related with the surface composition and structure of the catalyst samples. Surface property is influenced by bulk structure and preparation method of samples. Unfortunately, surface structure (including the variations of bond distance and angle relative to those in the bulk due to surface layer reconstruction, and also the surface defects formed after surface adsorbed species such as hydroxyl and carbonate group were desorbed upon heating) is not clear at atomic level at the present. Apparently, it is seen that as the La/Mn atomic ratio decreased, surface MnO*x* species aggregated gradually to form Mn_3O_4 phase at last. And the catalytic activity decreased with the La/Mn atomic ratio decreasing from 0.89 to 0.56. A further discussion will be given in Section 3.4. Similarly, La-deficient La–Fe perovskites were used as catalysts for methane oxidation in literatures [6,11]. An order in methane conversion of sample $La_{0.94}Fe > La_{0.83}Fe > La_{0.76}Fe > La_{0.64}Fe > La_{0.55}Fe$ (the atomic ratio of La/Fe was measured by ICP) was reported [6]. And an order of sample $La_{0.9}Fe > La_{0.8}Fe > La_{0.7}Fe > La_{1.0}Fe$ (the atomic ratio of La/Fe was nominal value of the fed chemicals) in methane conversion was also reported [11].

3.4. Further discussion for correlations with the La/Mn atomic ratio

In order to display more clearly effect of the La/Mn atomic ratio, several figures were drawn on the basis of Tables 1–3. Fig. 5 shows correlations of crystallite size of perovskite phase and specific surface area (SSA) of the La–Mn oxide samples with the La/Mn atomic ratio. It is clear that the La/Mn atomic ratio of 0.72 is a turning point, at which crystallite size of perovskite phase has the minimum value and specific surface area has the maximum value. The four samples with La/Mn atomic ratio at 1.03–0.72 are single phase perovskites, and the other two samples with La/Mn atomic ratio at 0.63 and 0.56 are mixture of perovskite with Mn_3O_4 phase according to XRD patterns. Due to the presence of Mn_3O_4 phase, the two samples with La/Mn atomic ratio at 0.63 and 0.56 have a relatively higher surface concentration of Mn element (by XPS) as shown in Fig. 6.

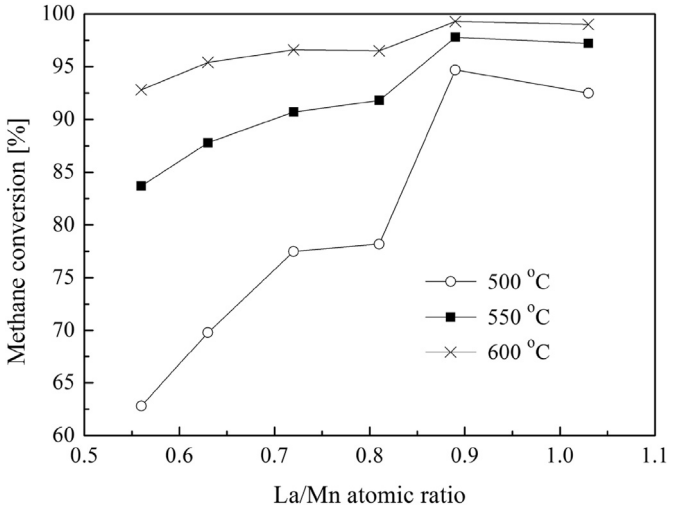

Fig. 4. Methane conversions as a function of the feed La/Mn atomic ratio at reaction temperatures of 500 °C, 550 °C and 600 °C.

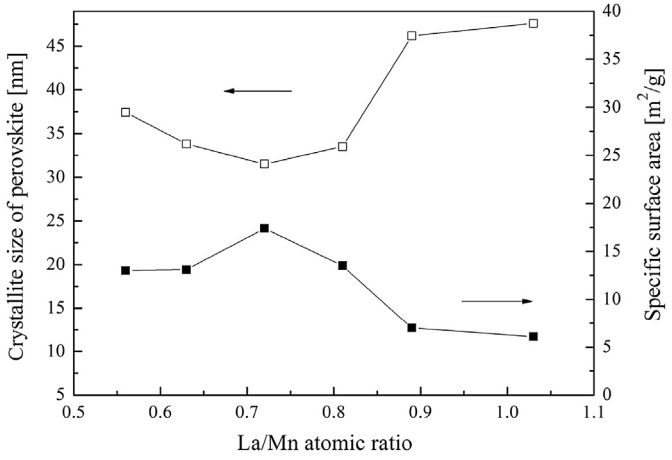

Fig. 5. Correlations of crystallite size of perovskite phase and specific surface area of the samples with the La/Mn atomic ratio.

Fig. 7 shows lattice vacancy at the A-sites (ϕ_A) and percentage of Mn^{4+} in the total Mn ions at the B-sites (i.e., $Mn^{4+}/(Mn^{3+} + Mn^{4+})$) of the perovskite phase. It is seen that as the La/Mn atomic ratio decreased from 1.03 to 0.72, lattice vacancy at the A-sites increased gradually to the maximum value due to the enlarged La-deficiency in the single phase of perovskite. Meanwhile, the percentage of Mn^{4+} at the B-sites also showed a maximum at the La/Mn atomic ratio of 0.72. Whereas, the lattice vacancy at the A-sites turned to decrease with the La/Mn atomic ratio further lowering to 0.63 and 0.56, because of Mn_3O_4 formed as a segregated phase at these two La/Mn atomic ratios. Correspondingly, the percentage of Mn^{4+} at the B-sites of perovskite decreased to a low value as well. It is worth noting that the samples with La/Mn atomic ratio at 1.03 and 0.89 exhibited notably higher percentage of Mn^{4+} at the B-sites. This should be associated with presence of lattice vacancy at the B-sites of the two samples. More Mn ions had to take valence state at +4 to compensate cationic lattice vacancies and maintain electrical neutrality of the crystal. In particular, the sample with La/Mn atomic ratio of 0.89 has a large number of lattice vacancies at the A-sites besides the vacancies at the B-sites, and thus has the highest percentage of Mn^{4+} among the six samples. It is stated that the number of high valence cation Mn^{4+} strongly influences methane oxidation activity [1]. This may provide an explanation for the activity order of the six samples for methane oxidation in Fig. 4, with

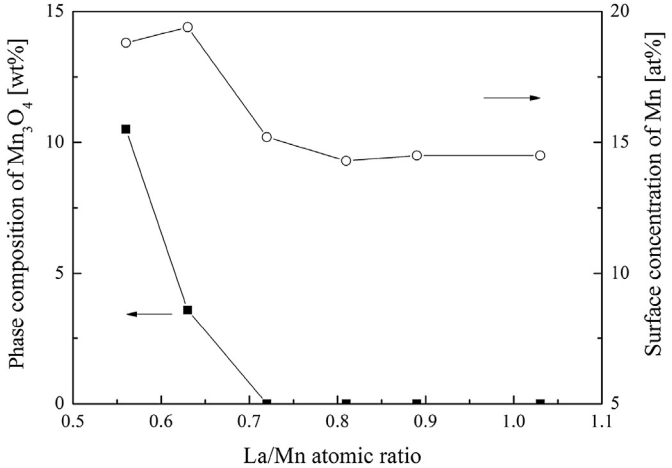

Fig. 6. Correlations of phase composition of Mn_3O_4 and surface concentration of Mn element of the samples with the La/Mn atomic ratio.

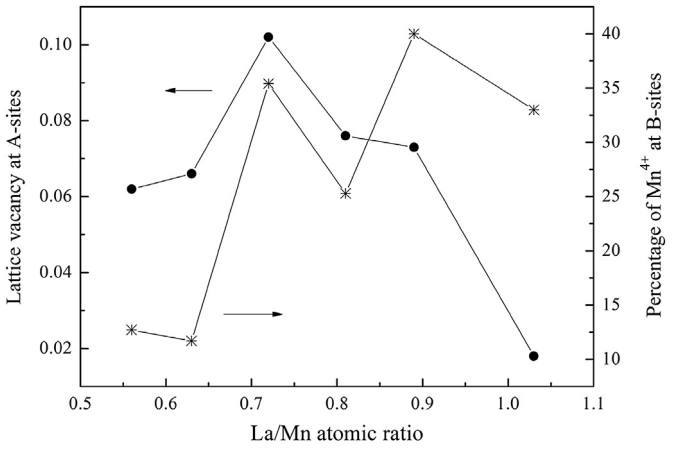

Fig. 7. Correlations of lattice vacancy at the A-sites and percentage of Mn^{4+} in total Mn ions at the B-sites of the perovskite phase with the La/Mn atomic ratio.

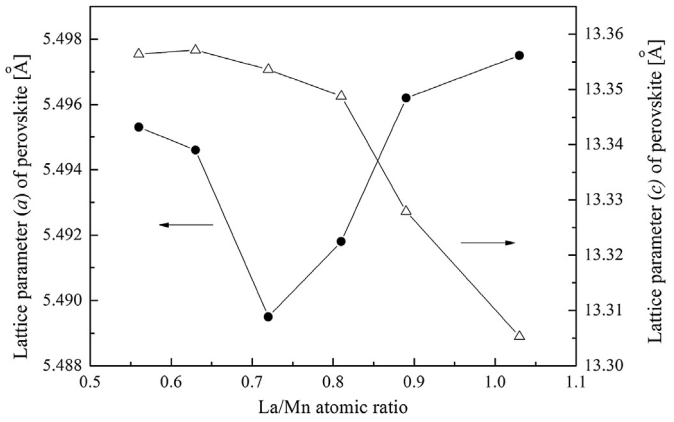

Fig. 8. Correlations of lattice parameter (a) and lattice parameter (c) of the perovskite phase with the La/Mn atomic ratio.

an exception at La/Mn atomic ratio of 0.72. The sample with La/Mn atomic ratio at 0.72 also has a larger number of Mn^{4+}, but shows a lower catalytic activity for methane oxidation. A possible reason may be that more part of surface of the sample was covered by the aggregated MnO*x* entity (which was not detectable by XRD), since the La/Mn atomic ratio of 0.72 is a turning point to form Mn_3O_4 phase upon La/Mn atomic ratio further decreasing. In addition, it is reported that apparent activation energy for methane oxidation is ca. 90 kJ/mol on a catalyst sample of $LaMnO_3$ calcined at 850 °C [1,8].

Fig. 8 shows variations of the lattice parameters of perovskite phase (on rhombohedral symmetry) with the La/Mn atomic ratio. It is seen that as the La/Mn atomic ratio decreases from 1.03 to 0.56, the parameter a decreases at first, reaches the smallest value and then increases again, meanwhile the parameter c exhibits an increasing tendency. Again, the La/Mn atomic ratio at 0.72 is a turning point in view of the parameter a, which coincides with the largest number of vacancy at the A-sites in Fig. 7, and the largest SSA value and the smallest crystallite size in Fig. 5. It is expected that value of the lattice parameters is dependent on numbers of lattice vacancy and Mn^{4+} ion in the crystal of perovskite phase.

4. Conclusions

The La–Mn oxide samples with feed La/Mn atomic ratio at 1.03, 0.89, 0.81 and 0.72 are all single phase perovskites. As the La/Mn atomic ratio lowers to 0.63 and 0.56, Mn_3O_4 phase is formed besides the main phase of perovskite. In all the six samples, highly dispersed MnO*x* species are present that are not detected by XRD. Lattice vacancy at the B-sites of the perovskites is likely to be present in the samples $La_{1.03}Mn$ and $La_{0.89}Mn$, and not in the other four samples. Lattice vacancy at the A-sites of the perovskites is present in all the six samples, in which the sample $La_{1.03}Mn$ has the smallest value due to La-sufficiency. There is an appreciable number of Mn^{4+} ions formed in the perovskite phase of the six samples, although the number is relatively smaller in the samples $La_{0.63}Mn$ and $La_{0.56}Mn$. Crystallite size of the perovskite phase is varying with the feed La/Mn atomic ratio, in consistence with specific surface area of the samples. Lattice parameters of the perovskite phase of the samples are also varying with the feed La/Mn atomic ratio. All these results indicate that the feed La/Mn atomic ratio affects crystal formation and growth of products in the solid reaction of preparation.

All the six samples are enriched with Mn ions on the surfaces. Catalytic activity for methane oxidation is in the order of sample $La_{0.89}Mn > La_{1.03}Mn > La_{0.81}Mn > La_{0.72}Mn > La_{0.63}Mn > La_{0.56}Mn$. The order is related with the surface composition and structure of the samples.

Acknowledgment

This work was financially supported by the National Natural Science Foundation of China (Grant No. 21171020).

References

[1] T. Seiyama, Total oxidation of hydrocarbons on perovskite oxides, Catal. Rev. – Sci. Eng. 34 (1992) 281–300.
[2] P. Ciambelli, S. Cimino, L. Lisi, M. Faticanti, G. Minelli, I. Pettiti, P. Porta, La, Ca, and Fe oxide perovskites: preparation, characterization and catalytic properties for methane combustion, Appl. Catal. B 33 (2001) 193–203.
[3] Z. Gao, R. Wang, Catalytic activity for methane combustion of the perovskite-type $La_{1-x}Sr_xCoO_{3-\delta}$ oxide prepared by the urea decomposition method, Appl. Catal. B 98 (2010) 147–153.
[4] G. Pecchi, P. Reyes, R. Zamora, C. Campos, L.E. Cadus, B.P. Barbero, Effect of the preparation method on the catalytic activity of $La_{1-x}Ca_xFeO_3$ perovskite-type oxides, Catal. Today 133–135 (2008) 420–427.
[5] B.P. Barbero, J.A. Gamboa, L.E. Cadus, Synthesis and characterization of $La_{1-x}Ca_xFeO_3$ perovskite-type oxide catalysts for total oxidation of volatile organic compounds, Appl. Catal. B 65 (2006) 21–30.
[6] J. Faye, A. Baylet, M. Trentesaux, S. Royer, F. Dumeignil, D. Duprez, S. Valange, J.-M. Tatibouet, Influence of lanthanum stoichiometry in $La_{1-x}FeO_{3-\delta}$ perovskites on their structure and catalytic performance in CH_4 total oxidation, Appl. Catal. B 126 (2012) 134–143.
[7] H. Tanaka, M. Uenishi, M. Taniguchi, I. Tan, K. Narita, M. Kimura, K. Kaneko, Y. Nishihata, J. Mizuki, The intelligent catalyst having the self-regenerative function of Pd, Rh and Pt for automotive emissions control, Catal. Today 117 (2006) 321–328.
[8] H. Arai, T. Yamada, K. Eguchi, T. Seiyama, Catalytic combustion of methane over various perovskite-type oxides, Appl. Catal. 26 (1986) 265–276.
[9] G. Pecchi, M.G. Jiliberto, A. Buljan, E.J. Delgado, Relation between defects and catalytic activity of calcium doped $LaFeO_3$ perovskite, Solid State Ionics 187 (2011) 27–32.
[10] C.-H. Wang, C.-L. Chen, H.-S. Weng, Surface properties and catalytic performance of $La_{1-x}Sr_xFeO_3$ perovskite-type oxides for methane combustion, Chemosphere 57 (2004) 1131–1138.
[11] A. Delmastro, D. Mazza, S. Ronchetti, M. Vallino, R. Spinicci, P. Brovetto, M. Salis, Synthesis and characterization of non-stoichiometric $LaFeO_3$ perovskite, Mater. Sci. Eng. B 79 (2001) 140–145.
[12] V.C. Belessi, P.N. Trikalitis, A.K. Ladavos, T.V. Bakas, P.J. Pomonis, Structure and catalytic activity of $La_{1-x}FeO_3$ system (x = 0.00, 0.05, 0.10, 0.15, 0.20, 0.25, 0.35) for the NO + CO reaction, Appl. Catal. A 177 (1999) 53–68.
[13] J.A.M. van Roosmalen, E.H.P. Cordfunke, R.B. Helmholdt, H.W. Zendbergen, The defect chemistry of $LaMnO_{3\pm\delta}$: 2. Structural aspects of $LaMnO_{3+\delta}$, J. Solid State Chem. 110 (1994) 100–105.
[14] R.V. Wandekar, B.N. Wani, D. Das, S.R. Bharadwaj, Preparation, characterization and the standard enthalpy of formation of $La_{0.95}MnO_{3+\delta}$ and $Sm_{0.95}MnO_{3+\delta}$, Thermochim. Acta 493 (2009) 14–18.
[15] Y. Zhang-Steenwinkel, J. Beckers, A. Bliek, Surface properties and catalytic performance in CO oxidation of cerium substituted lanthanum-manganese oxides, Appl. Catal. A 235 (2002) 79–92.

[16] S. Pence, M.A. Pena, J.L.G. Fierro, Surface properties and catalytic performance in methane combustion of Sr-substituted lanthanum manganites, Appl. Catal. B 24 (2000) 193–205.
[17] Y. Ng Lee, R.M. Lago, J.L.G. Fierro, V. Cortes, F. Sapina, E. Martinez, Surface properties and catalytic performance for ethane combustion of $La_{1-x}K_xMnO_{3+\delta}$ perovskites, Appl. Catal. A 207 (2001) 17–24.
[18] F. Patcas, F.C. Buciuman, J. Zsako, Oxygen non-stoichiometry and reducibility of B-site substituted lanthanum manganites, Thermochim. Acta 360 (2000) 71–76.
[19] E.R. Stobbe, B.A. de Boer, J.W. Geus, The reduction and oxidation behaviour of manganese oxides, Catal. Today 47 (1999) 161–167.
[20] A. Machocki, T. Ioannides, B. Stasinska, W. Gac, G. Avgouropoulos, D. Delimaris, W. Grzegorczyk, S. Pasieczna, Manganese-lanthanum oxides modified with silver for the catalytic combustion of methane, J. Catal. 227 (2004) 282–296.
[21] J.-C. Dupin, D. Gonbeau, P. Vinatier, A. Levasseur, Systematic XPS studies of metal oxides, hydroxides and peroxides, Phys. Chem. Chem. Phys. 2 (2000) 1319–1324.
[22] M.R. Goldwasser, M.E. Rivas, M.L. Lugo, E. Pietri, J. Perez-Zurita, M.L. Cubeiro, A. Griboval-Constant, G. Leclercq, Combined methane reforming in presence of CO_2 and O_2 over $LaFe_{1-x}Co_xO_3$ mixed-oxide perovskites as catalysts precursors, Catal. Today 107–108 (2005) 106–113.
[23] V. Di Castro, G. Polzonetti, XPS study of MnO oxidation, J. Electron Spectrosc. Relat. Phenom. 48 (1989) 117–123.